J Physiol Biochem (2015) 71:205–216
DOI 10.1007/s13105-015-0398-8

ORIGINAL PAPER

28-Day hindlimb unweighting reduces expression of Rho kinase and inhibits its effects in femoral artery of rat

Zhong-Chao Wang · Huan Liu · Yun-Gang Bai · Jin-Wen Yu · Hai-Jun Zhang · Yao-Ping Cheng · Jun-Xiang Bao · Xin-Ling Ren · Hong-Zhe Ma · Jin Ma

Received: 9 February 2014 / Accepted: 26 February 2015 / Published online: 12 March 2015

Abstract Previous studies have demonstrated inconsistent roles of Rho kinase (ROCK) in the decreased vasoconstriction of rat hindquarter vessels induced by hindlimb unweighting (HU). The present study was designed to determine the unclear role of ROCK in the mediation of HU-induced decreased femoral arterial vasoconstriction. 28-day HU rat was adopted as the animal model. With or without Y-27632, a ROCK inhibitor, isometric force of femoral artery was measured. The expression of ROCK and its effects on downstream targets were also examined. Results showed that (1) HU caused a significant decrease of the phenylephrine (PE)-evoked and potassium chloride (KCl)-evoked femoral arterial vasoconstriction ($P<0.05$), confirming the functional findings by previous studies. (2) Inhibition of ROCK with Y-27632 produced an equal reduction of the vasoconstriction in CON and HU. (3) HU significantly decreased ROCK II expression and the effects of ROCK on myosin light-chain phosphatase (MLCP) and MLC ($P<0.05$), but increased p65 nuclear translocation ($P<0.05$) and inducible nitric oxide synthase (iNOS) expression ($P<0.05$). (4) HU significantly ($P<0.05$) increased NO production in femoral arteries, with Y-27632 significantly ($P<0.01$) amplifying this effect. These findings have revealed that 28-day HU reduced the expression and effects of ROCK on downstream targets both directly (MLCP and MLC) and possibly indirectly (NF-κB/iNOS/NO pathway) related to vasoconstriction in femoral arteries.

Keywords Hindlimb unweighting · Femoral artery · Vasoconstriction · Rho kinase · Rat

Zhong-Chao Wang and Huan Liu contributed equally to this work.

Electronic supplementary material The online version of this article (doi:10.1007/s13105-015-0398-8) contains supplementary material, which is available to authorized users.

Z.-C. Wang · H. Liu · Y.-G. Bai · J.-W. Yu · H.-J. Zhang · Y.-P. Cheng · J.-X. Bao · H.-Z. Ma · J. Ma (✉)
Department of Aerospace Physiology, Fourth Military Medical University, No. 169, Changle West Road, Xi'an 710032, China
e-mail: jinmafmmu@163.com

J. Ma
e-mail: jin-ma@fmmu.edu.cn

X.-L. Ren
Department of Respiratory Diseases, Xijing Hospital, Fourth Military Medical University, Xi'an 710032, China

Introduction

Exposure to microgravity is one of the major threats encountered by astronauts during spaceflight. Among the various cardiovascular deconditioning effects induced by microgravity, postflight orthostatic intolerance is one of the most important concerns when astronauts return to earth [34, 35], but the true mechanism is still debatable. As one of microgravity-induced end-organ effects [34], abnormal vascular responsiveness has been reported in recent studies to be one of the possible explanations for the occurrence of postflight orthostatic intolerance.

Results from multiple human spaceflight [7] and bed rest studies [1, 2, 9] have demonstrated the adaptational

changes of the arterial vasculature in both real and simulated microgravity, which could possibly contribute to postflight orthostatic intolerance. Animal studies applying mice experiencing real spaceflight [28] and tail-suspended hindlimb unweighting (HU) rats [10, 18, 24, 34, 35] also give support to the involvement of microgravity-induced vascular responsiveness adaptations in postflight orthostatic intolerance. However, mechanisms underlying the aforementioned abnormal vascular responsiveness have not been fully elucidated.

As currently well accepted [4, 10, 14, 26, 27], the contraction of vascular smooth muscle cells (VSMCs) is mainly determined by the phosphorylation/dephosphorylation of myosin light chain (MLC), which is regulated by the balance between myosin light chain kinase (MLCK) and myosin light chain phosphotase (MLCP). In brief, a rise in cytosolic Ca^{2+} concentration produces VSMCs contraction by activation of Ca^{2+}-calmodulin-activated MLCK and subsequently phosphorylation of MLC, whereas activation of Ca^{2+}-independent MLCP could induce dephosphorylation of MLC and inhibit contraction. For many years, studies on the mechanisms of microgravity-induced abnormal vascular responsiveness mainly focused on iron channel-Ca^{2+} influx [5, 32], Ca^{2+} release [3, 33] and Ca^{2+}-calmodulin-activated MLCK pathway [16], yet few studies have paid attention to the Ca^{2+}-independent pathway.

It is now well established that MLC phosphorylation and VSMCs tension can be induced independently of the elevation of Ca^{2+} concentration, but directly through the increase in the sensitization of the contractile apparatus toward Ca^{2+}, which is mainly regulated by Rho-associated coiled-coil forming kinase (Rho kinase, ROCK) [14, 23, 30]. As documented by recent studies [8, 21], activated ROCK could phosphorylate MYPT-1, the regulatory subunit of MLCP and, in turn, inhibit MLCP activity and remain more MLC to be phosphorylated. Some other studies [14, 29] reported that ROCK could also directly phosphorylate MLC at Ser^{19} and exert contraction. Although ROCK has been proved to be involved in pathogenesis of various cardiovascular diseases, such as hypertension, atherosclerosis, and myocardial hypertrophy [4, 36], and is responsible for the tonic component of VSMCs in various vascular beds [14, 23, 30], if ROCK plays a role in the mediation of simulated microgravity-induced alterations of vascular responsiveness is still not fully understood.

Results from Li et al. [12] have indicated increased effect of ROCK by 14-day HU. However, in another study [27], decreased effect of RhoA/ROCK pathway was shown to be contributing to 20-day HU-induced decreased abdominal aortic vasoconstriction. Interestingly, previous studies [10, 18, 24] have consistently confirmed decreased responsiveness of both femoral artery and abdominal aorta in HU rats. Thus, the role of ROCK is still not clearly determined.

Since Li et al. only examined the effects of ROCK inhibition on vasoconstriction and speculated a compensatory activation of ROCK, the specific alterations of the expression and effects of ROCK in femoral arteries still need further investigation. Therefore, the present study adopted 28-day HU rats as the animal model to simulate medium-termed microgravity, examined effects of ROCK inhibition on femoral arterial vasoconstriction, and investigated ROCK expression and effects on downstream targets.

Materials and methods

Materials

Unless otherwise specially indicated, all the reagents and drugs seen below were purchased from Sigma-Aldrich (St. Louis, MO, USA) or Invitrogen Life Technologies (Carlsbad, CA, USA).

Animals and vascular tissue preparations

All experimental treatments and procedures involving animals were approved by the Institutional Animal Care and Use Committee of the Fourth Military Medical University, and in accordance with the guidelines for the care and use of animals required by the American Physiological Society.

Animals were supplied by the Laboratory Animal Centre of the Fourth Military Medical University. A total of 108 male Sprague–Dawley rats, 7–9 weeks of age and weighing between 260 and 280 g were randomly assigned to hindlimb unweighting (HU) and control (CON) group (n=54/group). To simulate the cardiovascular deconditioning effects seen in real/simulated microgravity, the HU rats were subjected to modified HU treatments for 28 days as previously described [13, 20]. The effect of HU was achieved by a tail harness to elevate the animal toward a head-down position with the hindlimbs suspended above the floor of the cage. The rats were maintained at ~35° head-down tilt with

the hindlimbs elevated ~0.5 cm above the floor. The HU rats were housed individually under a 12:12 h light/dark cycle at 23±1 °C with standard lab chow and water available ad libitum. Except for hindlimb unweighting, the CON rats received equal care as the HU animals, but housed in identical Plexiglas cages.

After 28-day HU, animals were anesthetized by intraperitoneal injection of pentobarbital sodium (40 mg/kg) and killed by exsanguination via the abdominal aorta. Then the bilateral femoral arteries were rapidly removed and placed in cold Krebs buffer solution consisting of (in mM): 118.3 NaCl, 4.7 KCl, 25 $NaHCO_3$, 1.2 $MgSO_4$, 1.2 KH_2PO_4, 2.5 $CaCl_2$, 11.1 glucose, and 0.026 EDTA (pH 7.4). After animal anatomy, arteries were carefully dissected from surrounding connective tissues and fats under a microscope. Artery rings were prepared for the isometric force measurement and the remains were snap frozen in liquid nitrogen and kept at −70 °C for Western blot analysis or homogenated immediately for ROCK activity assay.

For immunohistochemistry-staining studies, animals were perfused intracardially under deep anesthesia with isotonic sodium chloride solution, followed by 4 % paraformaldehyde in 0.1 mol/l sodium phosphate buffer at 4 °C (pH 7.4). Then the femoral arteries were isolated and cleaned as above, and artery rings (3 mm in length) were prepared and further fixed overnight in 4 % paraformaldehyde at 4 °C. Postfixed artery rings were embedded in paraffin, and 5 μm coronal sections were cut on a microtome for immunohistochemistry stain. For all the animals, the left wet weight of soleus and the relative muscle-body weight ratio were measured to confirm the efficacy of the animal model.

Isometric force measurement

The in vitro measurement of isometric force was implemented according to the methods described by Ma et al. [18] and Purdy et al. [24]. The femoral arteries were sectioned into artery rings 3 mm in length, and the endothelium was denuded by inserting a stainless steel needle into the lumen rubbing the inner face slightly. Then the rings were mounted onto two gracile stainless steel hooks and suspended in four chambered tissue bath (Radnoti, USA), with one hook attached to the tension transducer connecting to Powerlab (ADInstruments, Bella Vista NSW, Australia) for vasoreactivity recording, and the other to the plastic holder in the chamber. The chamber was filled with Krebs buffer solution, bubbled continuously with 95 % O_2–5 % CO_2 and kept at 37 °C. After equilibration for 30 min, rings were exposed to 60 mM KCl for stimulation and washed thoroughly back to the initial resting force till the optimal resting tension of 1 g [18, 24] was achieved.

After the course of preparations, concentration response curves (CRCs) evoked by PE or KCl were both obtained. In each experiment, rings were first exposed to accumulative addition of 10^{-10}–10^{-4} M PE or 10–100 mM KCl to stimulate force development. Then rings were incubated for 1 h with 3 μM Y-27632, a ROCK inhibitor, after which the dose-dependent contraction stimulated by PE or KCl was elicited again. The concentration of Y-27632 applied in this experiment was chosen according to the preliminary experiments and the work by Uehata et al. [30] and Summers et al. [27]. 50 % effective concentration (EC_{50}) was calculated to evaluate sensitivity of artery rings to vasoactive substances.

Western blot analysis

Homogenization and Western blot analysis were applied as previously described [17] to identify ROCK II, inducible NO synthase (iNOS), nuclear factor of kappa light polypeptide gene enhancer in B-cells inhibitor alpha (IκBα), and nuclear factor κB (NFκB) subunit p65 protein abundance, and phosphorylated MLC/total MLC ratio at Ser^{19}. The ROCK II isoform was investigated because it is most associated with MYPT-1 phosphorylation and VSMCs Ca^{2+} sensitization [4, 22]. Briefly, arteries were minced and homogenized on ice in tissue protein extraction reagent (Pierce, Rockford, IL, USA) containing protease inhibitor (Pierce) and phosphotase inhibitors (Roche, Basel, Switzerland) with the aid of a glass tissue grinder. Then the lysates were centrifuged at 12,000×*g* for 10 min at 4 °C, and the supernatants were collected. For nuclear p65 detection, an NE-PER Nuclear and Cytoplasmic Extraction Reagents kit (Pierce) was used, and experiment was conducted according to the instructions in the kit. Then protein concentrations were determined with a Bicinchoninic Acid Assay Kit (Pierce) with the standard of BSA. Equivalent amount of proteins were loaded to 4–12 % Bis–Tris PAGE gels under denaturing conditions within the NuPAGE Bis–Tris Pre-cast Gel System (Invitrogen Life Technologies). Then the fractionated proteins were electrophoretically transferred to polyvinylidene difluoride (PVDF) membranes

(Millipore, Billerica, MA, USA) in an XCell Blot Module transfer system (Invitrogen Life Technologies). After size separation, membranes were blocked for 6 h at room temperature with 5 % BSA in TBS containing 0.1 % (wt/vol) Tween 20 (TBS-T). Subsequently, membranes were incubated with mouse monoclonal antibody against phospho-MLC (Ser^{19}; 1:1000; Cell Signaling Technology, Boston, MA, USA), iNOS (1:200, Transduction Laboratories, San Diego, CA, USA) or rabbit polyclonal antibody against ROCK II (1:1000; Abcam, Cambridge, MA, USA), IκBα (1:1000, Cell Signaling Technology) and p65 (1:200, Santa Cruz, San Francisco, CA, USA) in TBS-T at 4 °C overnight, respectively. The membranes were washed six times with TBS-T and then incubated for 90 min at room temperature with horseradish peroxidase (HRP)-conjugated goat anti-mouse or anti-rabbit IgG (1:12000; Proteintech, Chicago, IL, USA) in TBS-T. A monoclonal mouse antibody against the structural protein β-actin or Lamin B1 was used as a lane-loading control. The bound antibodies were detected by enhanced chemiluminescence detection reagents (Millipore) in Gel Image Analyzing System (Tanon-4200, Tanon Science and Technology, Shanghai, China). After detection of phospho-MLC, the membrane was rinsed in stripping buffer (Beyotime Institute of Biotechnology, Shanghai, China) for 5 min and used to detect total MLC with the rabbit polyclonal antibody against MLC (1:1000; Cell Signaling Technology). Densitometry analysis of bands was performed by ImageJ software (National Institutes of Health, USA).

Immunohistochemistry

According to the manufacturer's instructions of the SP Histostain™-Plus Kits (ZYMED, San Diego, CA, USA), immunohistochemistry (IHC) was performed to further determine ROCK II abundance. Briefly, 5-μm sections prepared previously were deparaffinized with xylene and rehydrated by ethanol at graded concentrations and distilled water. High-temperature antigen retrieval was performed in 0.01 M citrate buffer, pH 6.0, in a microwave oven for 10 min. To block endogenous peroxidase activity, sections were incubated with 3 % H_2O_2 for 10 min. Subsequently, the sections were washed in PBS and then incubated with reagent A for 15 min at room temperature to block nonspecific antigen sites. Thereafter, sections were incubated with the rabbit polyclonal antibody against ROCK II (1:100) at 4 °C overnight, followed by rewarming at 37 °C for 30 min in the next morning. Then, sections were incubated with reagent B for 15 min at 37 °C. After three times wash with PBS, sections were incubated with reagent C under the same condition as reagent B. Finally, sections were incubated with the peroxidase substrate diaminobenzidine for 10 min, followed by slight counterstaining with hematoxylin, dehydration, and coverslipping with Permount TM Mounting Medium. Immunoreactivity was visualized and photographed using a microscope (Olympus BX51, Tokyo, Japan) at the appropriate wavelengths.

ROCK activity assay

The 96-well ROCK Activity Assay Kit (Cell Biolabs, San Diego, CA, USA) was applied to detect the specific ROCK activity. All procedures were conducted following the manufacturer's instructions in the kit. Briefly, as aforementioned, tissues were homogenated immediately after isolation with the recommended lysis buffer. After centrifugation, the supernatant was collected and diluted with kinase buffer once. Afterwards, the diluted tissue lysate samples or the active ROCK II positive control were added into the wells of the substrate plate. Kinase reaction was initiated by adding 10 μl of the ten times kinase reaction buffer containing DTT and ATP into each well. After incubation at 37 °C for 2 h, kinase reaction was stopped by flicking out the content in the wells. Then the wells were washed three times with 250 μl 1 × wash buffer with thorough aspiration between each wash, followed by incubation with 100 μl of the diluted anti-phospho-MYPT1 (Thr^{696}) antibody at room temperature for 2 h. After thorough wash as described above, wells were incubated with 100 μl of the diluted HRP-conjugated secondary antibody at room temperature for 2 h. Subsequently, after wash another three times, enzyme reaction was initiated by incubation with 100 μl of Substrate Solution for 30 min at 37 °C. Eventually, enzyme reaction was stopped by the addition of 100 μl of Stop Solution and the absorbance was read immediately on a spectrophotometer using 450 nm as the primary wavelength.

Nitric oxide (NO) assay

The Total Nitric Oxide Assay Kit (Beyotime Institute of Biotechnology) was applied to measure NO

concentration under several certain conditions. Experiments were conducted according to the instruction in the kit. Briefly, femoral arteries were collected and incubated with Y-27632 (3 μM), endothelial nitric oxide synthase (eNOS) inhibitor N^G-nitro-L-arginine methyl ester (L-NAME, 1 μM) or neuronal NOS (nNOS) inhibitor (4*S*)-*N*-(4-amino-5[aminoethyl]aminopentyl)-*N*′-nitroguanidine (NAAN, 240 nM) for 1 h in Krebs buffer at 37 °C. Then tissues were minced and homogenized on ice in recommended tissue protein extraction reagent (Beyotime Institute of Biotechnology). After centrifugation, supernatants were collected and protein concentration was measured as aforementioned. Then equivalent amount of proteins were loaded to 96-well plate, followed by addition of a series of reagents in accordance with the sequence recommended by the instruction. Since NO is not stable and could be quickly processed into nitrate and nitrite by cellular metabolism, we could calculate the total NO concentration through measuring the amount of nitrate and nitrite. As such, this kit adopted NADPH-dependent nitrate reductase method to reduce nitrate into nitrite, and detect nitrite with the classic Griess reagent. Finally, a spectrophotometer was used to read the absorbance at 540 nm as the relative nitrate and nitrite content.

Data analysis

Data are expressed as means±SE. Student's *t* test was used to determine the significance of differences in body weights, soleus wet weights, parallel muscle–body mass ratio, protein expression, and relative nitrate and nitrite content between groups. CRCs were analyzed by repeated-measures two-way ANOVA. Statistical analysis was performed using SPSS 16.0 (SPSS) software and Prism software 5.0 (Graphpad). A value of $P<0.05$ was considered to be statistically significant.

Results

Efficacy of animal model

During 28-day experimental period, all the animals grew well, and as summarized in Table 1, there were no significant differences in the initial or final body weights between CON and HU rats, suggesting a normal growth during simulated microgravity. However, compared with CON rats, HU significantly reduced the absolute left soleus wet weight at 48.1 % ($P<0.01$) and the relative soleus body weight ratio at 47.4 % ($P<0.01$), which confirmed the efficacy of simulated microgravity in this set of experiments.

Effects of HU and Y-27632 on femoral arterial contraction

The accumulative concentration-dependent tension development of the femoral arteries is presented in Fig. 1. As shown in Fig. 1a and b, HU significantly ($P<0.01$) reduced the maximal contraction evoked by both PE and KCl. Meanwhile, the femoral arterial vasoconstriction was also obtained in the presence of Y-27632. As shown in Fig. 1c and d, Y-27632 decreased the developed tension to lower levels in both CON and HU rats. As calculated in Fig. 1e and f, when expressed as the percentage of corresponding maximal contraction of CON or HU, the maximal tension of CON + Y-27632 or HU + Y-27632 evoked by both agonists was lowered by the same extent. Thus, Y-27632 exerted the same inhibitory effects on CON and HU femoral arterial vasoconstriction.

Effects of HU and Y-27632 on arterial vasoconstrictive sensitivity

As shown in Fig. 2, the values of EC_{50} were also computed. HU had no significant effect on the EC_{50} for either PE- or KCl-evoked contraction. However, Y-27632 significantly shifted the EC_{50} for both agonists to the right ($P<0.01$). Specifically, the EC_{50} values for PE-evoked contraction were shifted from 6.47±0.83 and 4.91±0.63×10^{-7} mol/l to 3.28±0.50 and 3.70±0.88×10^{-6} mol/l in CON and HU rats, respectively. Similarly, in KCl-evoked contraction, the EC_{50} values were increased from 38.99±0.37 and 37.89±0.81 mmol/l to 47.02±0.64 and 46.29±1.22 mmol/l in CON and HU rats, respectively.

Effects of HU on protein expression of ROCK II

Western blot analysis was conducted to detect the protein expression of ROCK II. As shown in Fig. 3a and b, HU significantly decreased the protein expression of ROCK II ($P<0.05$). In order to confirm this result, IHC staining was applied to determine the expression

Table 1 Body weight and wet weight of left soleus of CON and HU rats

Group	Body weight (g)		Wet weight of soleus	
	Initial	Final	Absolute (mg)	Relative body weight (mg/g)
CON	264.17±2.08	407.83±2.81	156.21±4.79	0.38±0.01
HU	265.80±2.49	402.77±3.01	81.08±3.16*	0.20±0.01*

Values are mean±SE; n=54 animals in each group

CON control, *HU* 28-day hindlimb unweighting

* $P<0.01$ vs. CON

and location of ROCK II in the vascular smooth muscle layers. Compared with CON (Fig. 3c), less positive staining alongside the vascular smooth muscle fibers were displayed in HU (Fig. 3d), indicating decreased expression of ROCK II by HU in the vascular walls.

Effects of HU on ROCK activity

Besides determining the expression of ROCK II in the femoral arteries, we further investigated the changes of ROCK activity induced by HU. A 96-well ROCK

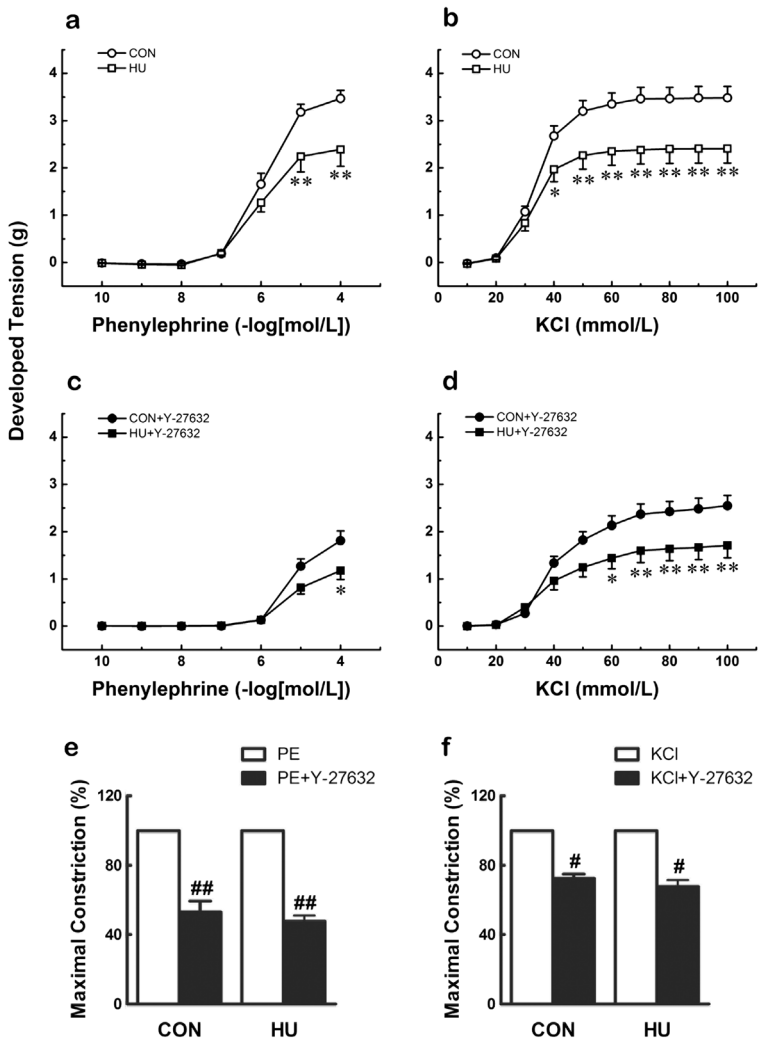

Fig. 1 Concentration response curves for vasoconstrictions to PE (**a** and **c**) or KCl (**b** and **d**) with (**c** and **d**) or without Y-27632 (**a** and **b**) from CON and HU rats. Statistical bar graphs depicting effects of Y-27632 on vasoconstriction to PE (**e**) or KCl (**f**). * $P<0.05$, ** $P<0.01$ vs. CON (**a**–**d**); # $P<0.05$, ## $P<0.01$ vs. absence of Y-27632 (**e** and **f**), n=10 in each group

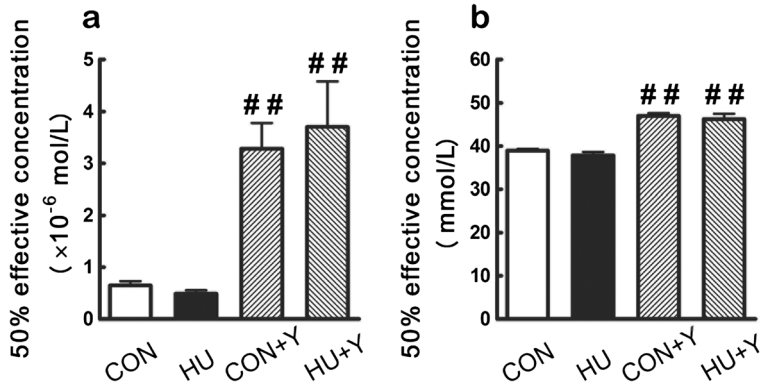

Fig. 2 EC_{50} of PE (**a**) and KCl (**b**) with or without Y-27632 from CON and HU rats. EC_{50}, 50 % effective concentration; CON + Y, control + Y-27632; HU + Y, hindlimb unweighting + Y-27632. $^{\#\#}P < 0.01$ vs. absence of Y-27632, $n = 10$ in each group

activity assay kit was used to detect the phosphorylative effect of ROCK on MYPT-1, a regulatory subunit of MLCP, at Thr^{696}. Anti-phospho-MYPT-1 (Thr^{696}) antibody was applied for the detection as described in the manufacturer's instructions. The results have shown that, as compared with CON (OD: 0.30±0.02), the absorbance was significantly reduced by HU (OD: 0.21±0.02) ($P < 0.05$), suggesting a decreased phosphorylative effect of ROCK on MYPT-1 at Thr^{696} by HU.

Western blot analysis was also performed to determine the phosphorylation level of MLC at Ser^{19}, another site directly phosphorylated by ROCK. As shown in Fig. 4, HU significantly ($P < 0.05$) increased the expression of MLC (Fig. 4b) but decreased the expression of phosphorylated MLC (p-MLC) at Ser^{19} (Fig. 4c). Thus, when normalized by total MLC, as shown in Fig. 4d, the level of p-MLC at Ser^{19} was further decreased by HU ($P < 0.01$), indicating less phosphorylative effect of ROCK on MLC at Ser^{19}.

Effects of HU on NFκB activation and iNOS protein expression

To examine the effects of HU on NFκB and iNOS, Western blot analysis was applied to detect the

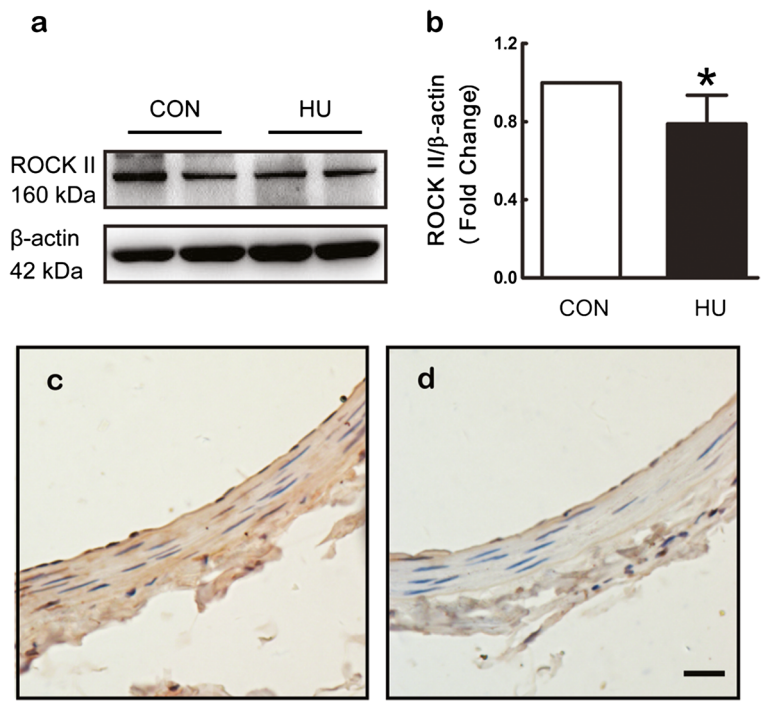

Fig. 3 Representative Western blots (**a**) and bar graphs (**b**) and immunohistochemistry photographs (**c** and **d**) depicting the protein expression of ROCK II in femoral arteries from CON (**c**) and HU (**d**) rats. Bar graph data are mean±SE of protein expression assayed in at least duplicate, quantified by densitometry, normalized to corresponding β-actin. Arteries for IHC were labeled with diaminobenzidine, which reacted with epitope of ROCK II conjugated with the primary and secondary antibodies, and produced brown staining. Original magnification, ×400. Bar, 100 μm. $^{*}P < 0.05$ vs. CON, $n = 7$ in each group

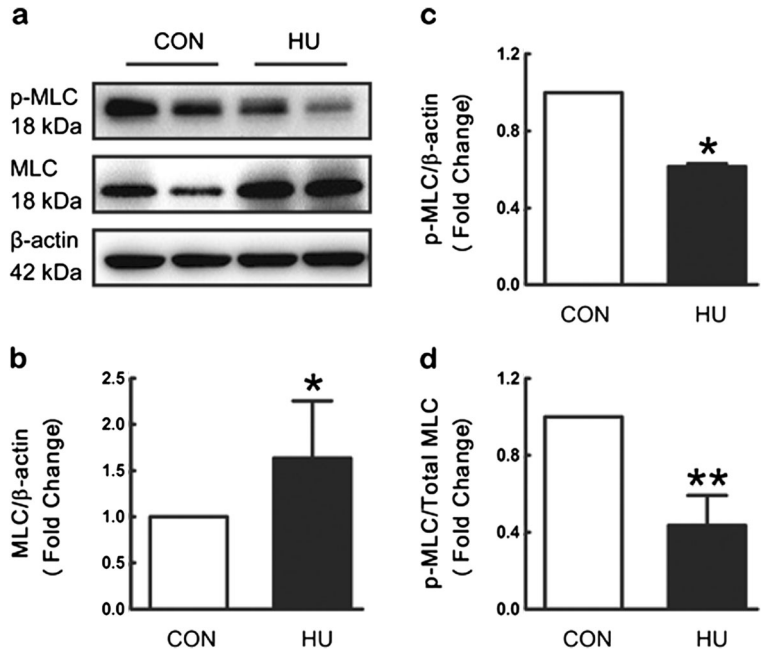

Fig. 4 Representative Western blots (**a**) and bar graphs (**b**, **c**, and **d**) depicting the protein expression of phospho/total MLC from CON and HU rats. Bar graph data are mean±SE of jprotein expression assayed in at least duplicate, quantified by densitometry, normalized to corresponding β-actin (**b** and **c**) or total MLC (**d**). *MLC* myosin light chain. $^{*}P<0.05$, $^{**}P<0.01$ vs. CON, $n=7$ in each group

expression of IκBα, total and nuclear p65, and iNOS. As shown in Fig. 5a, HU significantly suppressed the expression of IκBα ($P<0.01$) but had no significant influence on total p65 expression. To determine the nuclear translocation of NFκB, nuclear extraction of femoral artery tissues was performed and more nuclear p65 expression was detected in HU group (Fig. 5b, $P<0.05$), indicating activated NFκB nuclear translocation by HU. For the protein expression of iNOS, as shown in Fig. 5c, a band near 130 kDa was detected and iNOS expression was significantly increased by HU ($P<0.05$).

Effects of HU and Y-27632 on NO production

To determine NO production, we measured the relative nitrate and nitrite content with a total NO assay kit to represent the amount of NO in femoral artery tissues. As shown in Fig. 6, compared with CON, HU significantly increased the amount of NO by 1.3-folds ($P<0.05$). Meanwhile, Y-27632 alone further increased NO production by 1.8-folds in HU ($P<0.01$, vs. CON + Y-27632) but not CON group. Furthermore, application of Y-27632, L-NAME and NAAN together significantly ($P<0.01$) decreased NO content in both CON and HU, with the content 5.5-folds higher in HU than that in CON ($P<0.01$).

Discussion

The present study was designed to investigate the alterations of ROCK expression and effects on downstream targets and ROCK inhibition on vasoconstriction in femoral arteries induced by simulated microgravity. 28-day HU rats were adopted as the animal model to simulate the cardiovascular effects induced by simulated microgravity. The effects of Y-27632 on isometric force development, the protein expression of ROCK II, and the effects of ROCK on downstream targets were all examined in this study, and the key findings are as follows. (1) In consistent with the previous findings, HU induces impairment in the receptor-mediated and nonreceptor-mediated femoral arterial vasoconstriction. (2) Y-27632 reduces vasoconstriction in CON and HU to the same degree. (3) HU downregulates the protein expression of ROCK II and the phosphorylative effects of ROCK on MLCP and MLC. (4) HU upregulates the nuclear translocation of NFκB and the protein expression of iNOS. (5) HU increases NO production in femoral arteries, and Y-27632 amplifies this effect.

Since discovered in 1996, the extremely important role of ROCK in cardiovascular disease has been intensively studied [14]. Numerous studies [14, 15] have reported the involvement of ROCK in the regulation of abnormal vasoconstriction of various vascular types in many cardiovascular diseases, and the application of

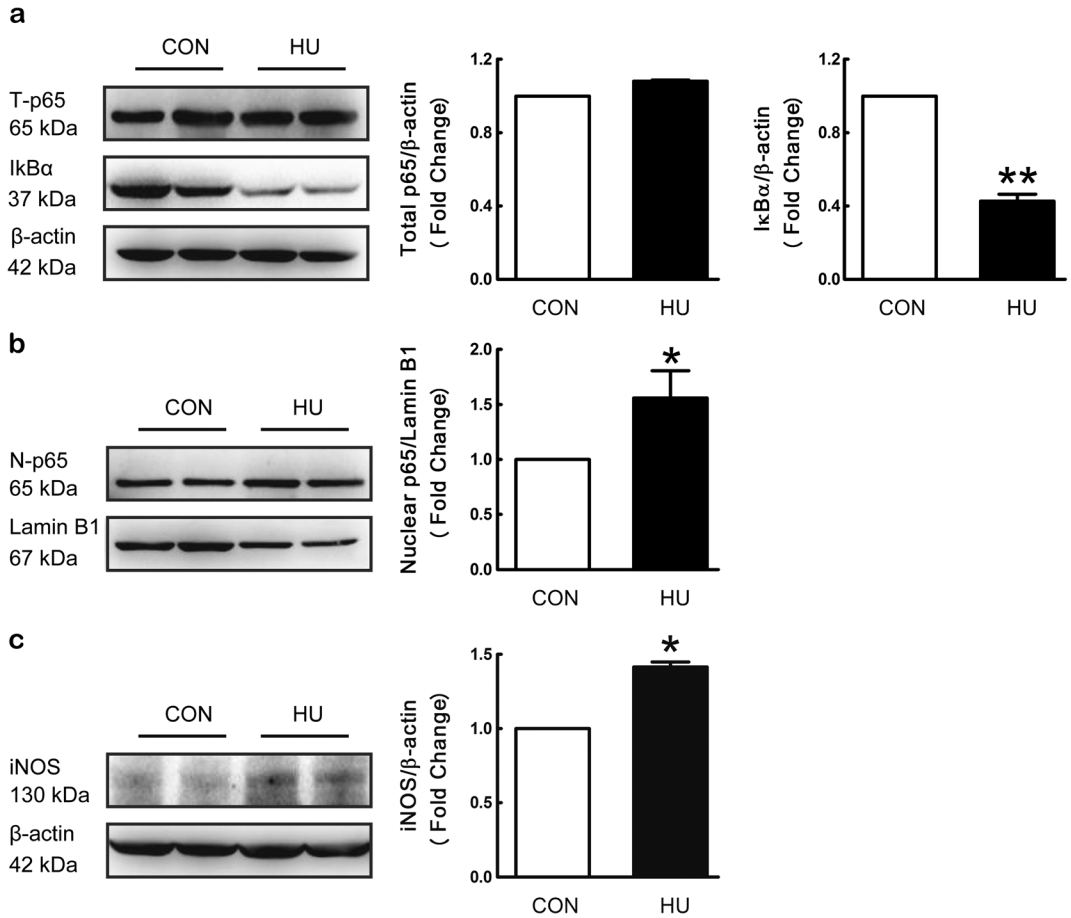

Fig. 5 Representative Western blots and bar graphs depicting the protein expression of total p65 and IκBα (**a**), nuclear p65 (**b**), and iNOS (**c**) from CON and HU rats. Bar graph data are mean±SE of protein expression assayed in at least duplicate, quantified by densitometry, normalized to corresponding β-actin (**a** and **c**) or Lamin B1 (**b**). *T-p65* total p65, *N-p65* nuclear p65. $^{*}P<0.05$, $^{**}P<0.01$ vs. CON, $n=6$ in each group

ROCK inhibitor could prevent the cardiovascular system from further pathologic changes [11]. Yet the role of ROCK in the mediation of altered vasoconstriction induced by real/simulated microgravity has not been intensively studied. As documented by previous studies [4, 6, 26], once activated by the upstream RhoA, ROCK could increase the sensitivity of VSMCs toward Ca^{2+} through its direct phosphorylative effects on MYPT-1, which, in turn, inhibits MLCP activity and reinforces VSMCs contraction. In some other studies [14, 29], the direct phosphorylative effect of ROCK on MLC at Ser^{19} was demonstrated to be another important pathway for ROCK to induce contraction. Thus, ROCK II expression and phosphorylation of its downstream targets, MYPT-1 at Thr^{696} and MLC at Ser^{19}, were examined in the present study. As shown by Western blot, IHC, and ROCK activity assay, decreased ROCK II expression and phosphorylation of the two targeted sites were demonstrated in our study, indicating decreased effects of ROCK by HU.

To determine if this inhibited ROCK is associated with HU-induced decreased femoral arterial vasoconstriction, effects of ROCK inhibition on vasoconstriction were tested. However, results have shown that Y-27632 reduced both PE- and KCl-evoked vasoconstriction to the same extent in CON and HU, indicating unchanged effects of ROCK by HU, which needs further explanation as follows.

Besides the role in regulating Ca^{2+} sensitization in VSMCs, ROCK has also been reported to be involved in the mediation of iNOS [25]. iNOS is barely detectable in normal vasculature but abundantly expressed by SMCs and macrophages under pathological conditions. Sangha et al. [25] have demonstrated that iNOS

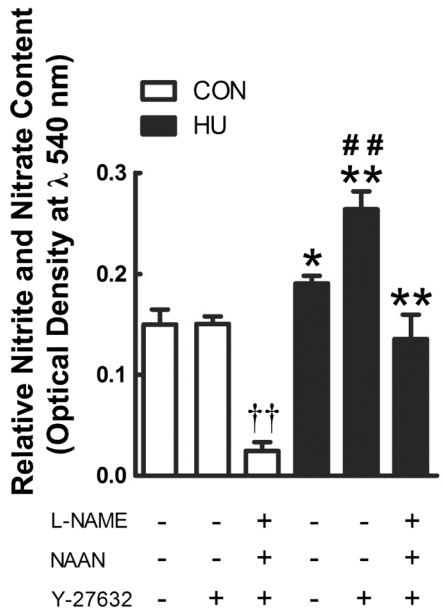

Fig. 6 Statistical bar graphs depicting the optical density at λ= 540 nm representing the relative nitrate and nitrite content in femoral arteries from CON, CON + Y-27632, CON + Y-27632 + L-NAME + NAAN, HU, HU + Y-27632, and HU + Y-27632 + L-NAME + NAAN group. $^{*}P<0.05$, $^{**}P<0.01$ vs. corresponding CON; $^{\#\#}P<0.01$ vs. absence of Y-27632 or presence of Y-27632 + L-NAME + NAAN (column 5 vs. column 4 or 6); $^{\dagger\dagger}P<0.01$ vs. absence of Y-27632 (column 3 vs. column 1), n=6 in each group

expression/activity may be increased in femoral arteries by 20-day HU, which could contribute to the vascular hyporesponsiveness to norepinephrine (NE). Yet the mechanism for this increased iNOS was unknown. As reviewed by Ma and Ma [19], NF-κB plays a key role in regulating iNOS gene expression. Moreover, previous studies [31] have also indicated a possible negative cross-talk between ROCK and IκB kinase (IKK)/NF-κB/iNOS pathway in VSMCs. Since the activation of NF-κB requires the degradation of IκB, an inhibitory protein of NF-κB, and the translocation of the p65 subunit from cytoplasm into nucleus, we detected the protein expression of IκBα and iNOS, the distribution of p65 subunit of NF-κB and the NO production in femoral arteries from 28-day HU rats to determine the possible involvement of NF-κB/iNOS/NO pathway. And we have demonstrated decreased IκBα expression and increased p65 nuclear translocation, indicating NF-κB activation by HU. Moreover, iNOS expression and NO production have also been shown to be increased by HU.

To establish the possible association between ROCK and NF-κB/iNOS/NO pathway, we examined the effects of ROCK inhibition on NO production. Results have shown that Y-27632 has further increased the NO production only in HU but not CON group, indicating that ROCK inhibition could amplify effects of HU on NO production. To further elucidate if this amplifying effect was associated with iNOS, we also applied eNOS inhibitor L-NAME and nNOS inhibitor NAAN. After the inhibition of the other two types of NOS, NO production was 5.5-folds higher in HU than that in CON group. Thus, 5.5-folds increase in NO production induced by HU + Y-27632 under the condition of eNOS and nNOS inhibition was much higher than 1.3-fold increase induced by HU alone, suggesting the effects of ROCK inhibition on NO production was regulated by iNOS.

Thus, a scenario could be concluded from the evidences above to at least partly explain the mechanisms underlying increased iNOS in the femoral artery by HU. 28-day HU may reduce the negative effects of ROCK on NF-κB in femoral artery, leading to more translocation of NF-κB from cytoplasm into nucleus and subsequent transcription reaction and iNOS expression. Increased iNOS expression could result in NO production, which may act as a vasodilator to reduce vasoconstriction. Moreover, the decreased femoral arterial vasoconstriction by HU could also be partly explained as follows. 28-day HU may have decreased the effects of ROCK, including phosphorylative effects on MLCP and MLC and possible negative effects on NF-κB/iNOS/NO pathway, both of which could lead to reduced femoral arterial vasoconstriction.

Finally, taken together (see Fig. S1), the equal inhibition of Y-27632 on the vasoconstriction in both groups on the basis of decreased ROCK by HU could be understood as follows. Since effects of ROCK on MLCP and MLC were decreased by HU, ROCK inhibition with Y-27632 would cause less decrease of the vasoconstriction in HU rats. However, Y-27632 could also block the remaining negative effects of ROCK on NF-κB/iNOS/NO pathway in HU rats, leading to further activation of NF-κB and subsequent increased iNOS expression. Consequently, NO production was increased and the femoral arterial vasoconstriction was further reduced in HU rats. Therefore, taken these two aspects into consideration, Y-27632 has caused an equal decrease of the femoral arterial vasoconstriction in CON and HU rats. However, the reason for the amplifying effect of Y-27632 on NO production existing only in HU, but not CON, group still needs further investigation.

Since one previous study [12] has demonstrated enhanced activity of ROCK induced by 14-day HU in femoral artery, together with results in the present study, we could only speculate ROCK as a possible compensatory effector in the beginning of HU to maintain the vascular responsiveness. But this compensatory mechanism could not persist along with the whole HU treatment period and, finally, decreased by HU at the time point in the present study. However, the time course of ROCK alterations induced by HU still merits further study.

Also, it should be noted that the protein expression of total MLC was increased by 28-day HU in the present study. A possible explanation could be provided as follows. As one of the downstream targets of ROCK, the expression of MLC could be regulated by ROCK alterations. Since 28-day HU has decreased the expression and effects of ROCK in the femoral arteries, a compensatory increase of the total expression of MLC could be induced as demonstrated in the present study. However, the effect of MLC is determined by its phosphorylation level, and increased expression of MLC could result in a relative decreased phosphorylation level of this protein. Thus, although expression of MLC was increased, it could not restore the decreased vasoconstriction. Nonetheless, we could not address this possibility with the present results, and future studies are needed to confirm this causal relationship.

In summary, the present study has demonstrated that 28-day HU reduced the expression of ROCK II, the phosphorylative effects of ROCK on MLCP at Thr^{696} and MLC at Ser^{19}, and the possibly negative effects on NF-κB/iNOS/NO pathway in femoral artery tissues. However, the mechanism underlying HU-induced alterations of ROCK requires further investigation.

Acknowledgments This study was supported by National Natural Science Foundation of China (Grant Nos. 31271279 and 30971423).

References

1. Arbeille P, Kerbeci P, Mattar L, Shoemaker JK, Hughson R (2008) Insufficient flow reduction during LBNP in both splanchnic and lower limb areas is associated with orthostatic intolerance after bedrest. Am J Physiol Heart Circ Physiol 295:H1846–H1854
2. Arbeille PP, Besnard SS, Kerbeci PP, and Mohty DM (2005) Portal vein cross-sectional area and flow and orthostatic tolerance: a 90-day bed rest study. J Appl Physiol (1985) 99: 1853–1857
3. Colleran PN, Behnke BJ, Wilkerson MK, Donato AJ, Delp MD (2008) Simulated microgravity alters rat mesenteric artery vasoconstrictor dynamics through an intracellular Ca(2+) release mechanism. Am J Physiol Regul Integr Comp Physiol 294:R1577–R1585
4. Denniss SG, Jeffery AJ, Rush JW (2010) RhoA-Rho kinase signaling mediates endothelium- and endoperoxide-dependent contractile activities characteristic of hypertensive vascular dysfunction. Am J Physiol Heart Circ Physiol 298: H1391–H1405
5. Fu ZJ, Xie MJ, Zhang LF, Cheng HW, Ma J (2004) Differential activation of potassium channels in cerebral and hindquarter arteries of rats during simulated microgravity. Am J Physiol Heart Circ Physiol 287:H1505–H1515
6. Fukuda S, Tsuchikura S, Iida H (2004) Age-related changes in blood pressure, hematological values, concentrations of serum biochemical constituents and weights of organs in the SHR/Izm, SHRSP/Izm and WKY/Izm. Exp Anim 53:67–72
7. Gazenko OG, Genin AM, Egorov AD (1981) Summary of medical investigations in the U.S.S.R. manned space missions. Acta Astronaut 8:907–917
8. Gokina NI, Park KM, McElroy-Yaggy K, and Osol G (2005) Effects of Rho kinase inhibition on cerebral artery myogenic tone and reactivity. J Appl Physiol (1985) 98: 1940–1948
9. Hughson RL, Shoemaker JK, Arbeille P, Dyson KS, Edgell H, Kerbeci P, Mattar L, Zuj K, Greaves DK (2007) WISE 2005: vascular responses to 60-day bed rest in women. J Gravit Physiol 14:P53–P54
10. Hwang S, Shelkovnikov SA, and Purdy RE (2007) Simulated microgravity effects on the rat carotid and femoral arteries: role of contractile protein expression and mechanical properties of the vessel wall. J Appl Physiol (1985) 102: 1595–1603
11. Kanda T, Hayashi K, Wakino S, Homma K, Yoshioka K, Hasegawa K, Sugano N, Tatematsu S, Takamatsu I, Mitsuhashi T, Saruta T (2005) Role of Rho-kinase and p27 in angiotensin II-induced vascular injury. Hypertension 45: 724–729
12. Li ZL, Yuan M, Jiang SZ, Wang DS, Wang HJ (2004) Role of ROK in contraction of rat femoral arteries after 14 d tail suspension. Space Med Med Eng (Beijing) 17:330–333
13. Lin LJ, Gao F, Bai YG, Bao JX, Huang XF, Ma J, Zhang LF (2009) Contrasting effects of simulated microgravity with and without daily -Gx gravitation on structure and function of cerebral and mesenteric small arteries in rats. J Appl Physiol 107:1710–1721
14. Loirand G, Guerin P, Pacaud P (2006) Rho kinases in cardiovascular physiology and pathophysiology. Circ Res 98:322–334
15. Loirand G, Pacaud P (2010) The role of Rho protein signaling in hypertension. Nat Rev Cardiol 7:637–647
16. Luo MZ, Li SS, Gao X, Lu Y, Yang ZQ, Zhang W, Shang P (2012) Effects of high magneto-gravitational environment on calcium/calmodulin signal of MG63 osteoblast-like cells. Xi Bao Yu Fen Zi Mian Yi Xue Za Zhi 28:225–227
17. Ma J, Kahwaji CI, Ni Z, Vaziri ND, Purdy RE (2003) Effects of simulated microgravity on arterial nitric oxide synthase and nitrate and nitrite content. J Appl Physiol 94:83–92
18. Ma J, Zhang LF, Yu ZB (1996) Effects of 14-day tail suspension on vasoreactivity of arteries from different parts of the body in rats. J Gravit Physiol 3:9–10

19. Ma S, Ma CC (2011) Recent development in pleiotropic effects of statins on cardiovascular disease through regulation of transforming growth factor-beta superfamily. Cytokine Growth Factor Rev 22:167–175
20. Morey-Holton ER, Globus RK (2002) Hindlimb unloading rodent model: technical aspects. J Appl Physiol (1985) 92: 1367–1377
21. Narumiya S, Ishizaki T, Watanabe N (1997) Rho effectors and reorganization of actin cytoskeleton. FEBS Lett 410:68–72
22. Noma K, Oyama N, Liao JK (2006) Physiological role of ROCKs in the cardiovascular system. Am J Physiol Cell Physiol 290:C661–C668
23. Pfitzer G (2001) Invited review: regulation of myosin phosphorylation in smooth muscle. J Appl Physiol (1985) 91: 497–503
24. Purdy RE, Duckles SP, Krause DN, Rubera KM, Sara D (1998) Effect of simulated microgravity on vascular contractility. J Appl Physiol 85:1307–1315
25. Sangha DS, Vaziri ND, Ding Y, and Purdy RE (2000) Vascular hyporesponsiveness in simulated microgravity: role of nitric oxide-dependent mechanisms. J Appl Physiol (1985) 88: 507–517
26. Somlyo AP, Somlyo AV (2003) Ca^{2+} sensitivity of smooth muscle and nonmuscle myosin II: modulated by G proteins, kinases, and myosin phosphatase. Physiol Rev 83:1325–1358
27. Summers SM, Nguyen SV, Purdy RE (2008) Hindlimb unweighting induces changes in the RhoA-Rho-kinase pathway of the rat abdominal aorta. Vasc Pharmacol 48:208–214
28. Taylor CR, Hanna M, Behnke BJ, Stabley JN, McCullough DJ, Davis RR, Ghosh P, Papadopoulos A, Muller-Delp JM, Delp MD (2013) Spaceflight-induced alterations in cerebral artery vasoconstrictor, mechanical, and structural properties: implications for elevated cerebral perfusion and intracranial pressure. FASEB J 27:2282–2292
29. Totsukawa G, Yamakita Y, Yamashiro S, Hartshorne DJ, Sasaki Y, Matsumura F (2000) Distinct roles of ROCK (Rho-kinase) and MLCK in spatial regulation of MLC phosphorylation for assembly of stress fibers and focal adhesions in 3T3 fibroblasts. J Cell Biol 150:797–806
30. Uehata M, Ishizaki T, Satoh H, Ono T, Kawahara T, Morishita T, Tamakawa H, Yamagami K, Inui J, Maekawa M, Narumiya S (1997) Calcium sensitization of smooth muscle mediated by a Rho-associated protein kinase in hypertension. Nature 389: 990–994
31. Wei CY, Huang KC, Chou YH, Hsieh PF, Lin KH, Lin WW (2006) The role of Rho-associated kinase in differential regulation by statins of interleukin-1beta- and lipopolysaccharide-mediated nuclear factor kappaB activation and inducible nitric-oxide synthase gene expression in vascular smooth muscle cells. Mol Pharmacol 69:960–967
32. Xie MJ, Ma YG, Gao F, Bai YG, Cheng JH, Chang YM, Yu ZB, Ma J (2010) Activation of BKCa channel is associated with increased apoptosis of cerebrovascular smooth muscle cells in simulated microgravity rats. Am J Physiol Cell Physiol 298:C1489–C1500
33. Xue JH, Chen LH, Zhao HZ, Pu YD, Feng HZ, Ma YG, Ma J, Chang YM, Zhang ZM, Xie MJ (2011) Differential regulation and recovery of intracellular Ca^{2+} in cerebral and small mesenteric arterial smooth muscle cells of simulated microgravity rat. PLoS One 6:e19775
34. Zhang LF (2013) Region-specific vascular remodeling and its prevention by artificial gravity in weightless environment. Eur J Appl Physiol 113:2873–2895
35. Zhang LF (2001) Vascular adaptation to microgravity: what have we learned? J Appl Physiol (1985) 91: 2415–2430
36. Zhou Q, Liao JK (2009) Rho kinase: an important mediator of atherosclerosis and vascular disease. Curr Pharm Des 15: 3108–3115